Performance of Different Types of FRCM Composites Applied to a Concrete Substrate

Tommaso D'Antino[1], Jaime Gonzalez-Libreros[2(✉)], Carlo Pellegrino[2], Christian Carloni[3], and Lesley H. Sneed[4]

[1] Department of Architecture, Built Environment, and Construction, Politecnico Di Milano, Milan, Italy
[2] Department of Civil, Environmental, and Architectural Engineering, University of Padua, Padua, Italy
jaime.gonzalez@dicea.unipd.it
[3] Department of Civil, Chemical, Environmental, and Materials Engineering, University of Bologna, Bologna, Italy
[4] Department of Civil, Architectural, and Environmental Engineering, Missouri University of Science and Technology, Rolla, MO, USA

Abstract. This research aimed to investigate the performance of fiber reinforced cementitious matrix (FRCM) composites employed as externally applied strengthening system for reinforced concrete members. The results of an experimental campaign conducted on FRCM composites applied to a concrete substrate are shown and discussed. The composites were comprised of different types of fibers, namely carbon, glass, steel, and basalt fibers, and different types of cementitious matrix. Single-lap direct-shear tests were performed to study the behavior of the different composites. Specimens with different bonded lengths were tested to investigate the stress-transfer mechanism and to investigate the existence of an effective bond length. Comparisons between the peak loads obtained with the direct-shear tests and the tensile strength of the fibers, which provide an indication of the exploitation of the fibers, were carried out.

Keywords: FRCM · Bond · Single-lap shear tests · Strengthening

1 Introduction

In recent decades the use of fiber reinforced polymer (FRP) composites in strengthening existing structures has gained great popularity. FRP composites have numerous advantages, such as their ease of application, high strength-to-weight ratio, and very limited volume occupancy. Nevertheless, FRP composites present some drawbacks related to the use of organic binders, such as poor resistance to relatively high temperature, difficulty in applying onto wet substrates, and poor compatibility with the substrate. To overcome these issues, new composite materials that employ inorganic binders and high strength fibers have been recently developed. Although other names can be found in the literature (Hartig et al. 2011; Tzoura and Triantafillou 2016),

V. Mechtcherine et al. (eds.), *Strain-Hardening Cement-Based Composites*,
RILEM Bookseries 15, DOI 10.1007/978-94-024-1194-2_89

composite materials that employ inorganic matrices and high strength fibers are usually referred to as fiber reinforced cementitious matrix (FRCM) composites. FRCM composites can be comprised of different types of fibers (e.g. carbon, glass, steel, PBO, or basalt fibers) that are embedded within specific types of matrix. FRCM composites are particularly interesting for strengthening and retrofitting of heritage buildings because of their compatibility with the substrate and their reversibility character (Valluzzi et al. 2014). Although FRCM composites have been applied to existing structures (D'Ambrisi et al. 2015), limited studies are available in the literature, and no European design guidelines exist as of yet. FRCM composites have been proven to be effective in flexural strengthening (Pellegrino and D'Antino 2013), shear strengthening (Tzoura and Triantafillou 2016), and confinement of axially/eccentrically loaded RC elements (Bournas and Triantafillou 2011; Ombres 2014). When applied for flexural or shear strengthening, FRCM composites comprised of one layer of fibers are reported to fail due to debonding (D'Ambrisi et al. 2013; Sneed et al. 2014, 2015), whereas either fiber fracture or debonding may occur in confinement applications (Triantafillou et al. 2006).

In this study the bond behavior of FRCM composites comprised of different types of fibers, namely steel, glass, carbon, and basalt fibers, applied to concrete supports were investigated through the use of a single-lap direct-shear test set-up. Different bonded lengths and a specific bonded width for each composite were used to investigate the existence of an effective bond length. The effectiveness of each composite material in fully exploiting the fiber strength is evaluated through comparison between the peak loads obtained with the direct-shear tests and the tensile strength of the fibers. The results analyzed herein were part of different experimental campaigns and are compared in this paper to provide an insight into the different behaviors and failure modes that can be obtained with various FRCM composites.

2 Experimental Campaign

FRCM-concrete joints comprised of steel, glass, carbon, and basalt fibers were tested. Glass, carbon, and basalt fibers were bundled and arranged in the form of a balanced net with bundles spaced at 20 mm, 25 mm, and 25 mm, respectively, whereas steel fibers were comprised of only longitudinal 5-filament strands with a nominal cross-sectional area equal to 240 mm^2/m. Carbon fiber bundles were bare, whereas glass and basalt fiber bundles were coated to improve the adhesion with the matrix and, in the case of glass fibers, to provide alkali-resistance. The steel strands were comprised of brassed ultra high tensile strength steel (UHTSS) filaments.

The tensile strength of each fiber type was determined by testing a minimum of three coupon specimens. Each specimen was comprised of n bare fiber bundle(s) 500 mm long. The tensile tests were conducted in displacement control at a rate of 0.5 mm/min following ASTM D3039 (ASTM 2008). The peak tensile strength σ_t^* was computed as $P_t^*/(nA_b)$ where P_t^* is the peak load attained and A_b the area of a single strand/bundle. Tensile specimens were named following the notation FK_Y_Z, where F indicates the fiber employed (S = steel, G = glass, C = carbon, B = basalt), K indicates the area weight of the fiber net in g/m^2, Y = width of the specimen in mm,

Table 1. Fiber strength.

Name	n	A_b [mm^2]	$\sigma^*_{t,avg}$ [MPa] (CoV)
S190_60_1-3	33	0.48	3350 (0.066)
G250BA_4_1-5	1	1.25	720 (0.024)
C170BL_4_1-4	1	0.94	1260 (0.033)
B350BA_4_1-3	1	1.45	1150 (0.051)

and Z = specimen number. The average tensile strengths $\sigma^*_{t,avg}$ obtained for each type of fiber is reported in Table 1.

Matrix W was used for steel FRCM composites, and Matrix S was employed for all other FRCM composites. Specimens with Matrix W were cast in one batch, whereas those with Matrix S were cast in four batches. Although each batch was prepared in the same manner and the specimens were cured in the same way, the matrix mechanical properties slightly varied for Matrix S. At least three 40 mm × 40 mm × 160 mm samples were cast from each matrix batch used to prepare the FRCM and tested according to UNI EN 1015-11 (UNI 2007). The average flexural strength f_{flex} and average compressive strength r_{cm} obtained for each batch are reported in Table 2.

Table 2. Matrix strength.

Name	Batch	f_{flex} [MPa] (CoV)	r_{cm} [MPa] (CoV)
S	A	3.60 (0.176)	16.70 (0.091)
	B	4.50 (0.034)	17.10 (0.022)
	C	3.90 (0.047)	11.40 (0.022)
	D	6.50 (0.065)	24.80 (0.051)
W	–	6.40 (0.009)	47.60 (0.040)

Compressive tests according to UNI EN 12390-3 (UNI 2009) were carried out on six 150 mm cubes cast from the same batch used to cast the concrete blocks used for the FRCM-concrete joints. The average compressive strength was 59.3 MPa (CoV = 0.150).

The composite strips were applied to concrete blocks (prisms) with 125 mm × 125 mm cross-section and 500 mm length, which were restrained to the machine base (Fig. 1).

The concrete faces were sandblasted before applying the glass, carbon, and basalt FRCM composites, whereas they were simply cleaned before the application of steel FRCM composites. Each FRCM-concrete joint was comprised of one layer of fibers embedded within two 4 mm thick matrix layers. Glass and carbon fiber nets outside the bonded length were impregnated with epoxy resin in an attempt to distribute the load and avoid premature failure (D'Antino et al. 2015a). Two LVDTs were mounted on the sides of the composite strip near the loaded end. For glass, carbon, and basalt FRCM-concrete joints the displacement measured by an additional LVDT mounted on the middle of an Ω–shaped aluminum plate bonded to the concrete block approximately 20 mm from the loaded end was used to control the tests that were conducted at a constant rate equal to 0.008 mm/s. The steel FRCM-composite joints were tested in

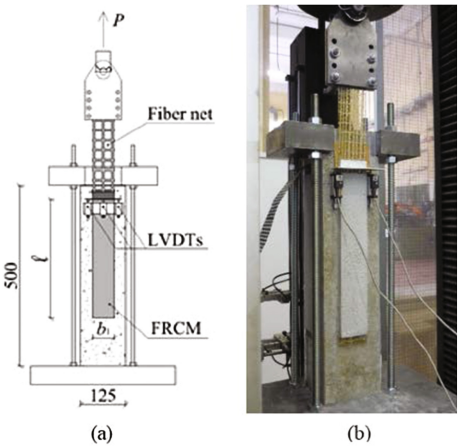

Fig. 1. (a) Test set-up for glass, carbon, and basalt FRCM-concrete joints. (b) Specimen DS_S190W_330_60_1.

stroke control at a rate of 0.005 mm/s. The 2 + 1 (where present) LVDTs reacted off of a thin aluminum L–shaped plate bonded to the fibers just outside the bonded length.

3 Results

Experimental Load Responses. A total of 42 FRCM-concrete joints were tested. For brevity, only a summary of the results obtained is provided in this section; further details can be found in (D'Antino et al. 2015a, b; Gonzalez et al. 2015).

Four different bonded lengths ℓ (100 mm, 200 mm, 330 mm, and 450 mm) were tested for glass, carbon, and basalt FRCM composites, whereas two bonded lengths (330 mm and 450 mm) were tested for steel FRCM composites. Carbon and basalt FRCM composites included $n = 3$ longitudinal fiber bundles and had a bonded width b_1 equal to 60 mm and 75 mm, respectively. Glass and steel FRCM composites included $n = 3$ longitudinal fiber bundles ($b_1 = 55$ mm) and $n = 33$ steel strands ($b_1 = 60$ mm), respectively. Specimens were named following the notation DS_FMK_X_Y_Z, where F = fiber employed (S = steel, G = glass, C = carbon, B = basalt), M = matrix employed (W = matrix W, S = matrix S), K indicates the area weight of the fiber net in g/m^2, X = bonded length (ℓ) in mm, Y = bonded width (b_1) in mm, and Z = specimen number. Figure 2a summarizes the applied load P versus global slip g responses of the specimens with carbon FRCM composites. All specimens with carbon FRCM composites failed due to debonding, which occurred at the fiber-matrix interface, and was characterized by significant slippage of the fibers (Fig. 2b). Comparing specimens with bonded lengths of 330 mm and 450 mm, Fig. 2a shows only a slight increase in peak load (average of 6.4%). Accordingly, the effective bond length should be less than 450 mm, however further results are needed to determine its exact value. Additionally, because the composites were cast in different batches and had different mechanical characteristics, the results show no significant

Table 3. Results of single-lap direct-shear tests.

Name	σ^* [MPa]	$\sigma^* / \sigma^*_{t,avg}$	Batch	Name	σ^* [MPa]	$\sigma^* / \sigma^*_{t,avg}$	Batch
DS_CS17BL_100_60_1	270	0.21	A	DS_BS350_450_75_2	380	0.33	D
DS_CS17BL_100_60_2	200	0.16	A	DS_GS25BA_100_55_1	130	0.18	B
DS_CS17BL_100_60_3	150	0.12	A	DS_GS25BA_100_55_2	210	0.29	B
DS_CS17BL_100_60_4	150	0.12	C	DS_GS25BA_100_55_3	170	0.24	B
DS_CS17BL_200_60_1	310	0.25	A	DS_GS25BA_100_55_4	170	0.24	C
DS_CS17BL_200_60_2	340	0.27	A	DS_GS25BA_200_55_1	180	0.25	B
DS_CS17BL_200_60_3	270	0.21	A	DS_GS25BA_200_55_2	330	0.46	B
DS_CS17BL_330_60_1	560	0.44	A	DS_GS25BA_200_55_3	280	0.39	B
DS_CS17BL_330_60_2	560	0.44	A	DS_GS25BA_200_55_4	340	0.47	C
DS_CS17BL_330_60_3	440	0.35	A	DS_GS25BA_330_55_1	470	0.65	B
DS_CS17BL_330_60_4	580	0.46	C	DS_GS25BA_330_55_2	460	0.64	B
DS_CS17BL_450_60_1	610	0.48	A	DS_GS25BA_330_55_3	530	0.74	B
DS_CS17BL_450_60_2	660	0.52	A	DS_GS25BA_450_55_1	550	0.77	B
DS_CS17BL_450_60_3	550	0.44	A	DS_GS25BA_450_55_2	550	0.77	B
DS_BS350_100_75_1	120	0.10	D	DS_GS25BA_450_55_3	630	0.88	B
DS_BS350_100_75_2	150	0.13	D	DS_SW190_330_60_1	630	0.55	–
DS_BS350_200_75_1	300	0.26	D	DS_SW190_330_60_2	370	0.32	–
DS_BS350_200_75_2	240	0.21	D	DS_SW190_330_60_3	250	0.22	–
DS_BS350_330_75_1	380	0.33	D	DS_SW190_450_60_1	460	0.40	–
DS_BS350_330_75_2	340	0.30	D	DS_SW190_450_60_2	280	0.24	–
DS_BS350_450_75_1	460	0.40	D	DS_SW190_450_60_3	400	0.35	–

influence on the load responses. This proves that the matrix mechanical properties do not play a fundamental role in the load-carrying capacity, also referred to as the debonding load (Carloni et al. 2015).

Figure 2c summarizes the *P-g* curves for the specimens with glass FRCM composites. All specimens with glass FRCM composites failed due to fiber debonding from the embedding matrix (Fig. 2d). Fiber rupture within or just outside the bonded area, which was associated with drops in the *P-g* curves in Fig. 2c, was observed for certain specimens after debonding. For short bonded lengths (i.e., 100 and 200 mm), there was no post-peak descending branch of the load response, which indicates that the contribution of friction was larger than the contribution of bond for these specimens. Similar to the carbon FRCM composite specimens, variations in matrix mechanical properties did not significantly influence the load responses.

Figure 3a summarizes the *P-g* curves for the specimens with steel FRCM composites. For most specimens, brittle detachment of the composite strip at the matrix-concrete interface was observed (Fig. 3b). For the case of specimen DS_SW190_450_60_1, matrix interlaminar failure (delamination) occurred (Fig. 3c). It should be noted that surface treatment could improve the matrix-substrate bond properties to preclude composite detachment at the matrix-concrete interface.

Figure 3d summarizes the *P-g* curves for the specimens with basalt FRCM composites, which failed due to debonding at the matrix-fiber interface. For specimens with

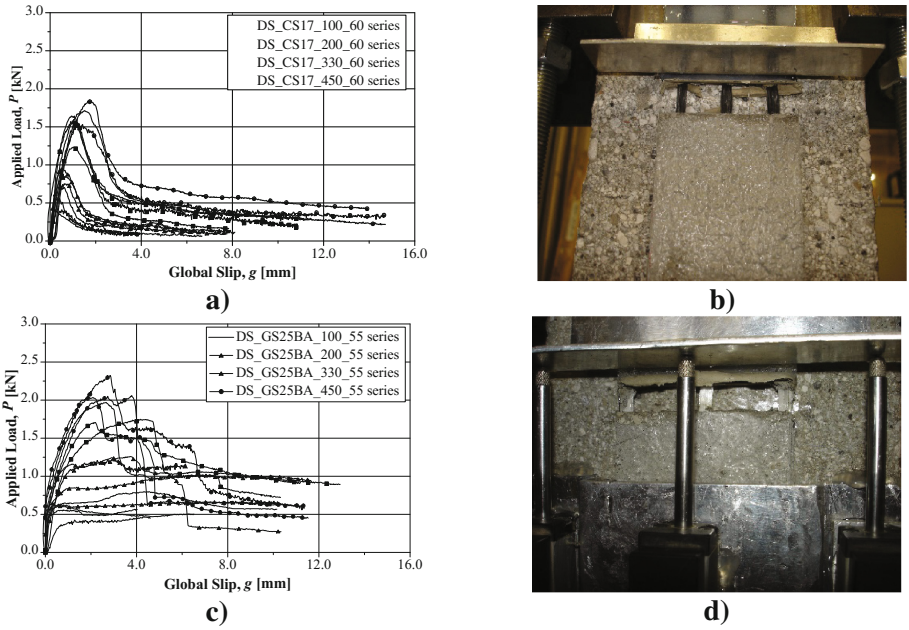

Fig. 2. (a) Load responses of FRCM-concrete joints with carbon fibers. (b) Photo of specimen DS_CS17BS_450_60_3 after failure. (c) Load responses of FRCM-concrete joints with glass fibers. (d) Photo of specimen DS_GS25BA_450_55_3 after failure.

bonded length less than or equal to 330 mm the *P-g* was similar to those of glass FRCM composites with bonded lengths of less than or equal to 200 mm described above, which indicates that the friction between the basalt fibers and the embedding matrix was generally larger than the contribution of bond. Sudden drops in the basalt FRCM *P-g* curves were associated with failure of one or more fiber bundles within the matrix (Fig. 3d).

Fiber Exploitation in FRCM Composites. Since failure of FRCM-concrete joints is generally reported to be debonding at the matrix-fiber interface, the strength of the fibers is usually not fully exploited. To determine the effectiveness of different types of FRCM composites in exploiting the fiber strength, the load-carrying capacity (debonding load) obtained with shear tests should be compared with the fiber tensile strength. It should be noted, however, that the debonding load depends not only on the stress-transfer mechanism, but it is also affected by the presence of friction between matrix and fiber and between fiber filaments (D'Antino et al. 2014). Since the debonding load is not easily determined, the peak load P^* (or peak stress σ^*) can be compared with the fiber tensile strength as a first attempt to obtain an indication of the fiber exploitation for different bonded lengths. The ratio between the peak stress obtained from shear tests σ^* and the average fiber tensile strength $\sigma^*_{t,avg}$ (Table 1) is reported in Table 3 for each specimen. Comparing specimens with the same matrix (Matrix S) and ℓ = 450 mm, it can be observed that the glass FRCM composite is

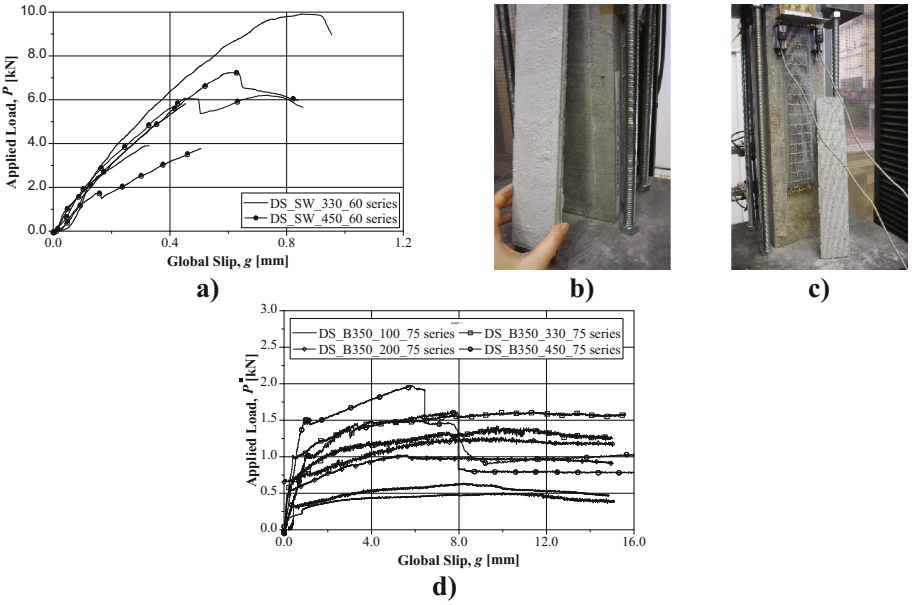

Fig. 3. (a) Load responses of FRCM-concrete joints with steel fiber. Photo of specimen (b) DS_SW190_330_60_2 and (c) DS_SW190_450_60_1 after failure. (d) Load responses of FRCM-concrete joints with basalt fiber.

capable of better exploiting the fiber strength, attaining a maximum value of $\sigma^*/\sigma^*_{t,avg} = 0.88$, whereas carbon and basalt FRCM composites attained a maximum of 0.52 and 0.40, respectively. The steel FRCM composites reported a maximum value of $\sigma^*/\sigma^*_{t,avg} = 0.55$ for $\ell = 330$ mm. Since steel FRCM composites failed due to debonding at the matrix-substrate interface or splitting at the matrix-fiber interface, their behavior should not be compared with that of other FRCM composites that reported different failure modes.

4 Conclusion

This paper provided an overall view of the results obtained from 42 single-lap direct-shear tests of different FRCM composites. FRCM composites employed were comprised of carbon, glass, basalt, and steel fibers. Different bonded lengths and one specific bonded width for each composite were employed. Except for steel FRCM composites, specimens were cast with the same matrix on different days exhibiting different values of the matrix flexural and compressive strength. However, the different mechanical characteristics of the matrix did not appear to affect the load responses.

Specimens cast with Matrix S failed due to debonding at the matrix-fiber interface. The peak load values increased at different rates with increasing bonded length, suggesting the existence of an effective bond length for these composites.

When compared with the fiber tensile strength, glass FRCM composites were reported to be the most effective in exploiting the fiber tensile strength, having a ratio $\sigma^*/\sigma^*_{t,avg}$ equal to 0.88 for bonded length ℓ = 450 mm.

Steel FRCM composites, which were applied on untreated concrete surface (only cleaned), failed due to debonding at the matrix-substrate interface or delamination at the matrix-fiber interface. Treating the concrete surface might prevent failure at the composite-substrate interface.

References

ASTM International. Standard test method for tensile properties of polymer matrix composite materials. ASTM D3039/D3039M-08, West Conshohocken, PA (2008)

Bournas, D.A., Triantafillou, T.C.: Bar buckling in RC columns confined with composite materials. J. Compos. Constr. **15**(3), 393–403 (2011)

Carloni, C., D'Antino, T., Sneed, L.H., Pellegrino, C.: Role of the matrix layers in the stress-transfer mechanism of FRCM composites bonded to a concrete substrate. J. Eng. Mech. **141**(6), 04014165 (2015)

COMITÉ EUROPÉEN DE NORMALIZATION. Methods of test for mortar for masonry—Part 11: determination of flexural and compressive strength of hardened mortar. UNI EN 1015-11, Brussels (2007)

COMITÉ EUROPÉEN DE NORMALIZATION. Testing hardened concrete. Compressive strength of test specimens. UNI EN 12390-3, Brussels (2009)

D'Ambrisi, A., Feo, L., Focacci, F.: Experimental analysis on bond between PBO-FRCM strengthening materials and concrete. Compos. Part B: Eng. **44**(1), 524–532 (2013)

D'Ambrisi, A., Focacci, F., Luciano, R., Alecci, V., De Stefano, M.: Carbon-FRCM materials for structural upgrade of masonry arch road bridges. Compos. Part B: Eng. **75**, 355–366 (2015)

D'Antino, T., Carloni, C., Sneed, L.H., Pellegrino, C.: Matrix-fiber bond behavior in PBO FRCM composites: a fracture mechanics approach. Eng. Frac. Mech. **117**, 94–111 (2014)

D'Antino, T., Pellegrino, C., Carloni, C., Sneed, L.H.: Experimental analysis of the bond behavior of glass, carbon, and steel FRCM composites. Key Eng. Mat. **624**, 371–378 (2015a)

D'Antino, T., Pellegrino, C., Carloni, C., Sneed, L.H.: Experimental investigation of glass and carbon FRCM composite materials applied onto concrete supports. In: Proceedings 2nd International Symposium Advances in Civil and Infrastructure Engineering, 12–13 June. Vietri sul Mare, Italy (2015b)

Gonzalez, J., D'Antino, T., Pellegrino, C.: Bond behaviour of basalt FRCM composite applied on RC elements. In: Proceedings 3rd Conference Smart Monitoring, Assessment and Rehabilitation of Civil Structures, 7–9 September. Antalya, TR (2015)

Hartig, J., Jesse, F., Schicktanz, K., Häußler-Combe, U.: Influence of experimental setups on the apparent uniaxial tensile load-bearing capacity of textile reinforcement concrete specimens. Mat. Struc. **45**, 433–446 (2011)

Ombres, L.: Concrete confinement with a cement based high strength composite material. Compos. Struct. **109**, 294–304 (2014)

Pellegrino, C., D'Antino, T.: Experimental behaviour of existing precast prestressed reinforced concrete elements strengthened with cementitious composites. Compos. Part B: Eng. **55**, 31–40 (2013)

Sneed, L.H., D'Antino, T., Carloni, C.: Investigation of bond behavior of PBO fiber-reinforced cementitious matrix composite-concrete interface. ACI Mat. J. **111**(1–6), 1–12 (2014)

Sneed, L.H., D'Antino, T., Carloni, C., Pellegrino, C.: A comparison of the bond behavior of PBO-FRCM composites determined by single-lap and double-lap shear tests. Cem. Conc. Compos. **64**, 37–48 (2015)

Tzoura, E., Triantafillou, T.C.: Shear strengthening of reinforced concrete T-beams under cyclic loading with TRM or FRP jackets. Mat. Struc **49**, 17–28 (2016)

Triantafillou, T.C., Papanicolaou, C.G., Zissinopoulos, P., Laourdekis, T.: Concrete confinement with textile-reinforced mortar jackets, ACI Struct. J. **1**(103), 28–37 (2006)

Valluzzi, M.R., Modena, C., De Felice, G.: Current practice and open issues in strengthening historical buildings with composites. Mat. Struct. **47**, 1971–1985 (2014)